Fully gapped superconductivity in In-doped topological crystalline insulator Pb_{0.5}Sn_{0.5}Te

Guan Du, Zengyi Du, Delong Fang, Huan Yang, R. D. Zhong, J. Schneeloch, G. D. Gu, and Hai-Hu Wen

Phys. Rev. B **92**, 020512 — Published 27 July 2015

DOI: 10.1103/PhysRevB.92.020512

Fully gapped superconductivity in In-doped topological crystalline insulator $Pb_{0.5}Sn_{0.5}Te$

Guan Du[1], Zengyi Du[1], Delong Fang[1], Huan Yang[1*], R. D. Zhong[2], J. Schneeloch[2], G. D. Gu[2], and Hai-Hu Wen[1*]
[1] *National Laboratory of Solid State Microstructures and Department of Physics, Collaborative Innovation Center of Advanced Microstructures, Nanjing University, Nanjing 210093, China and*
[2] *Condensed Matter Physics and Materials Science Department, Brookhaven National Laboratory, Upton, New York 11973, USA*

Superconductors derived from topological insulators and topological crystalline insulators by chemical doping have long been considered to be candidates as topological superconductors. $Pb_{0.5}Sn_{0.5}Te$ is a topological crystalline insulator with mirror symmetry protected surface states on (001), (011) and (111) oriented surfaces. The superconductor $(Pb_{0.5}Sn_{0.5})_{0.7}In_{0.3}Te$ is produced by In doping in $Pb_{0.5}Sn_{0.5}Te$, and is thought to be a topological superconductor. Here we report the first scanning tunneling spectroscopy measurement of the superconducting state as well as the superconducting energy gap in $(Pb_{0.5}Sn_{0.5})_{0.7}In_{0.3}Te$ on a (001)-oriented surface. The spectrum can be well fitted by an anisotropic s-wave gap function of $\Delta(\theta) = 0.72 + 0.18\cos 4\theta$ meV using Dynes model. The results show that the superconductor seems to be a fully gapped one without any in-gap states, in contradiction with the expectation of a topological superconductor.

PACS numbers: 74.55.+v, 74.20.Mn, 74.20.Rp, 74.90.+n

Topological superconductors (TSC) have been predicted as a new phase of matter, and are topologically distinct from conventional superconductors[1]. As a manifestation of their peculiar properties, topological superconductors host solid-state realizations of Majorana fermions at their boundaries which obey non-Abelian statistics and have potential value of realizing topological quantum computation[2].

Seeking for new TSC has already been a very hot spot. One method to obtain topological superconductivity is to construct topological insulator/conventional superconductor heterostructures[3–8]. Topological insulators (TI) are cousins of TSC with insulating bulk states and metallic surface states protected by time-reversal symmetry[9], and topological superconductivity can be induced in TI by superconducting proximity effect[3]. Superconductors derived from TI by doping have also been considered as candidates, e.g., $Cu_xBi_2Se_3$[10] is predicted to be the TSC theoretically[11]. Point contact measurements have detected zero-bias conductance peaks (ZBCP)[12,13] which are interpreted to be signatures of Majorana fermions[14,15]. However the ZBCP are absent in normal metal/superconductor junction with finite barriers[16] and scanning tunneling spectroscopy (STS) measurements[17].

Another interesting system to search TSC is the superconductor derived from topological crystalline insulators (TCI) by doping. TCI are topologically nontrivial states of matter in which the topological nature of electronic structures arises from crystal symmetries[18]. Examples of TCIs have been found in the IV-VI semiconductor SnTe[19,20], and substitutional solid solutions $Pb_{1-z}Sn_zTe$[21,22] and $Pb_{1-z}Sn_zSe$[23–25]. $Pb_{1-z}Sn_zTe$ undergoes a transition from a trivial insulator to a TCI when z exceeds 0.3[26]. The (001), (011) and (111) oriented surfaces of these TCI are mirror symmetric about {011} mirror planes and have an even number of Dirac cones[27–29], which is quite different from TI. Superconductivity has been found in In doped SnTe[30,31], and is considered to be topologically nontrivial[30]. ZBCP have been detected by point contact measurements in $Sn_{1-x}In_xTe$ and are also interpreted as signatures of nontrivial topological superconductivity[32]. However, some groups reported later that their data do not support the conclusion of a novel superconductor[33,34]. Whether the superconductivity in doped TCI is topologically nontrivial is still unknown. Superconductivity was also found in In doped $Pb_{1-z}Sn_zTe$[35–41], and this material is a new possible candidate for TSC according to former theoretical proposals[32]. The quality of $(Pb_{1-z}Sn_z)_{1-x}In_xTe$ crystals and the superconducting transition temperature has been improved recently[42], and T_c reaches maximum 4.7 K at its optimum doping of $x = 0.3$. To verify its topological properties accurately, detecting the gap structure is strongly called for.

STS is a direct probe to detect the local density of states (LDOS), which can provide key and intrinsic information on the superconducting gap symmetry[43,44]. In this Rapid Communication, we present the first measurements of the local tunneling spectra on optimally doped $(Pb_{1-z}Sn_z)_{1-x}In_xTe$ and results of its superconducting gap structure.

We chose $(Pb_{0.5}Sn_{0.5})_{0.7}In_{0.3}Te$ for the present investigation, and Sn content of $z = 0.5$ makes it sure that the parent compound is topologically nontrivial as referred above[26]. The high-quality single crystal was grown by the floating-zone method[42]. The DC magnetic susceptibility was measured using a commercial Magnetic Property Measurement System (SQUID-VSM, Quantum Design). The resistivity was measured using the standard four-probe configuration performed on Physical Property Measurement System (PPMS, Quantum Design).

The crystal structure of $(Pb_{0.5}Sn_{0.5})_{0.7}In_{0.3}Te$ is similar to sodium chloride. Here Pb, Sn and In atoms share the same kind of sites in the lattice. The (001)-

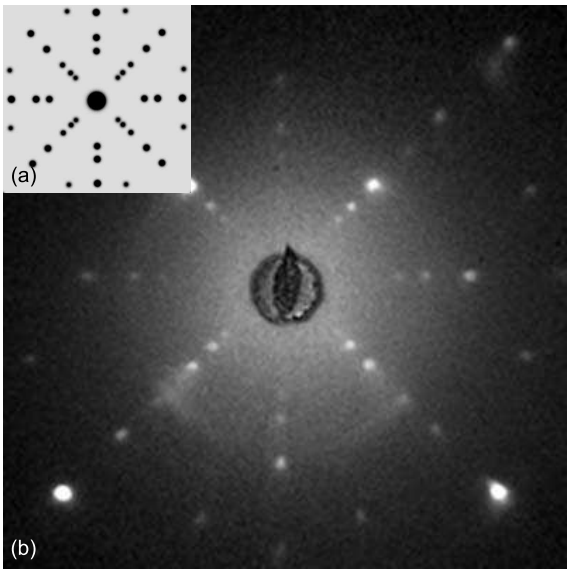

FIG. 1: (color online) (a) Theoretically simulated Laue diffraction patterns of (001)-oriented surface of $(Pb_{0.5}Sn_{0.5})_{0.7}In_{0.3}Te$. (b) Experimental Laue diffraction patterns from the cleaved surface of a single crystal.

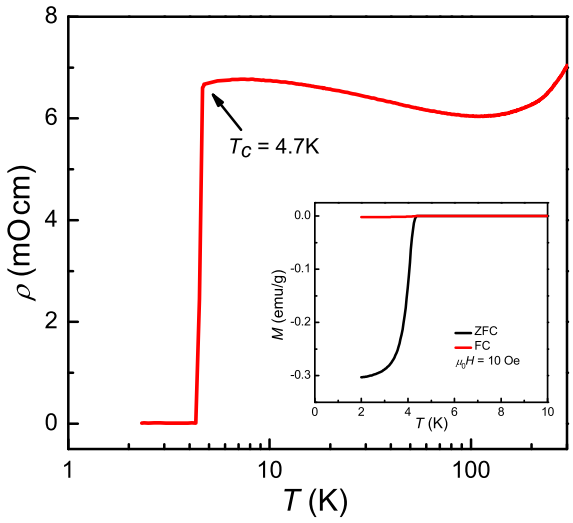

FIG. 2: (color online) Temperature dependence of the resistivity in semi-log plot for a $(Pb_{0.5}Sn_{0.5})_{0.7}In_{0.3}Te$ single crystal. The inset shows the temperature dependence of magnetic susceptibility measured with ZFC and FC processes at an applied field of 10 Oe.

oriented planes are naturally cleavage planes, and are mirror symmetric about {011} mirror planes. In parent compound topological crystalline insulator $Pb_{0.5}Sn_{0.5}Te$, such kind of surfaces host topologically nontrivial surface states[27]. Therefore identifying the (001) crystal orientation in the first place is very necessary in order to detect underlying features of the superconductivity in $(Pb_{0.5}Sn_{0.5})_{0.7}In_{0.3}Te$. Lacking of natural crystal surfaces, we polished the crystal and got a smooth surface. Then Laue x-ray crystal alignment system (Photonic Science Ltd.) was used to investigate the orientation of the crystal according to the Laue diffraction patterns. Fig. 1(a) shows the theoretical simulation of Laue diffraction patterns when the x-ray perpendicular to the (001)-oriented surface, and obviously it has the fourfold symmetry which is consistent with the crystal structure. We adjusted the incidence angle of the x-ray until fourfold symmetric patterns came into view. Then the crystal was polished again according to the former step. After repeating several times, new patterns were obtained as shown in Fig. 1(b) when the x-ray was applied perpendicular to the top surface. Since they agree well with the theoretical simulation, the obtained top surface is confirmed to be (001)-oriented. Then the $(Pb_{0.5}Sn_{0.5})_{0.7}In_{0.3}Te$ crystal was cleaved in the ultra-high vacuum chamber with pressure better than 10^{-10} torr at $\sim$ 80 K. The resultant tiny surfaces with the scale of sub-millimeters and different height are usually (001)-oriented. Then the cleaved sample was quickly transferred to the scanning tunneling microscope (STM) head. The STM/STS measurements were carried out with an ultra-high vacuum, low temperature and high magnetic field scanning probe microscope USM-1300 (Unisoku Co., Ltd.). $Pb_{1-z}Sn_zSe$ crystal seems very easy to cleave and is usually atomically resolved on the cleaved surface[45–47]. However for $(Pb_{0.5}Sn_{0.5})_{0.7}In_{0.3}Te$ the cleavage made many tiny (001)-oriented surfaces, and the measured surfaces usually have the roughness of about several angstroms which may result from the indium doping. The STS spectra were measured by a lock-in amplifier with an ac modulation of 0.1 mV at 987.5 Hz to lower down the noise.

The main panel in Fig. 2 shows the temperature dependence of the electrical resistivity for a $(Pb_{0.5}Sn_{0.5})_{0.7}In_{0.3}Te$ single crystal. One can find that temperature dependent resistivity increases with the temperature decreasing from 110 K to 7 K. This semiconductor like behavior is rare for superconductors, and may be inherited from the insulating behavior in the parent compound of $Pb_{0.5}Sn_{0.5}Te$. The superconducting transition occurs at about 4.7 K with a narrow transition width, indicating the high quality of the sample. The inset of Fig. 2 shows the temperature dependence of magnetic susceptibility and the superconducting transition occurs at about 4.5 K characterized by the zero-field-cooled (ZFC) process and field-cooled (FC) process at 10 Oe.

We applied STS measurements on the newly cleaved (001)-oriented surface at the temperature of 400 mK. A typical spectrum is shown in Fig. 3(a) covering a voltage

range of ±4 mV, and it is symmetrical to the zero-bias in the presented range. The superconducting gap appears near the Fermi level with pronounced coherence peaks located at ±0.9 mV. The 'U'-shape instead of a 'V'-shape of the bottom near the zero bias suggests a nodeless superconducting gap existing in the material. The differential conductance value at zero-bias is about 0.07 with relative to the value at higher bias voltage outside coherence peaks, indicating that the LDOS within the energy of superconducting gaps are almost fully gapped. The remaining finite zero-bias LDOS is due to slight broadening effect, which will be discussed later. Odd paring symmetries are predicted theoretically for TSC, and the bulk LDOS can be either fully gapped or gapped with point node/line node(s) by tuning the chemical potential and the effective mass of the energy band[14,15]. The surface Andreev bound states appear as the form of the helical Majorana fermions in the bulk quasi-particle gap. This kind of in-gap states has several kinds of structure in the energy dispersions, such as cone, caldera, ridge, or valley shaped[15]. In any cases, they give rise to zero-bias LDOS significantly on the surface. Therefore, the zero-bias peaks should be viewed in the tunneling conductance measurements as a signature of the nontrivial superconductivity. In addition, the coherence peaks are even absent because of the sharp and broad zero-bias peak from the theoretical calculation[14], which contrasts sharply with an s-wave superconductor. However, those features are not viewed in our measurements.

In order to verify the paring symmetry of $(Pb_{0.5}Sn_{0.5})_{0.7}In_{0.3}Te$, we fitted the data with several scenarios of superconducting gaps based on the Dynes model[48] as shown in Figs. 3(b)–(f). The measured differential conductance (dI/dV) was normalized by the value at bias voltage of 4 mV far from the coherence peaks. Then the experimental conductance was fitted with tunneling current for one gap of

$$I(V) \propto \int_{-\infty}^{\infty} d\varepsilon \int_{0}^{2\pi} d\theta [f(\varepsilon) - f(\varepsilon + eV)] \times \mathrm{Re}\left\{ \frac{\varepsilon + eV - i\Gamma}{[(\varepsilon + eV - i\Gamma)^2 - \Delta^2(\theta)]^{1/2}} \right\}, \quad (1)$$

where Γ is the broadening parameter, $f(\varepsilon)$ is the Fermi distribution function which contains the thermal broadening effect at some finite temperature, and the temperature parameter used for fitting is the same as the experimental temperature. The results based on pure s-wave and d-wave fittings are plotted with the experimental data in Figs. 3(b) and 3(c) respectively. The pure s-wave fitting to the spectrum yields a superconducting gap value of $\Delta = 0.77$ meV and broadening parameter of $\Gamma = 0.07$ meV. And for pure d-wave fitting, $\Delta = 0.9$ meV, $\Gamma = 0.005$ meV. Both of the two fitting results fail to track the low energy feature, i.e., the s-wave fitting displays a more flat bottom near the Fermi energy while the d-wave fitting appears to be not flat enough. In addition the coherence peaks of both two fitting results

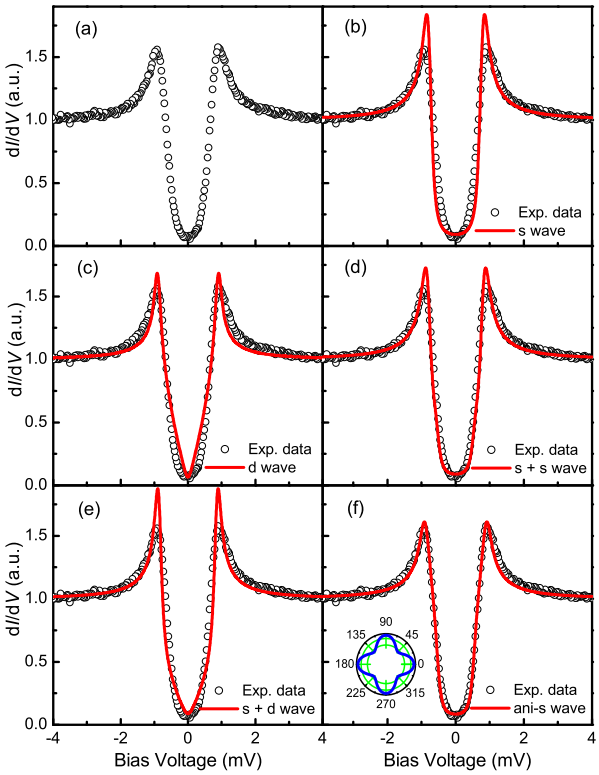

FIG. 3: (color online) (a) A typical STS spectrum measured at 400 mK. The fitting results are shown in (b)–(f). The symbols represent the experimental data, and the colored lines are the theoretical fits to the data with Dynes model by (b) s-wave, (c) d-wave, (d) double s-waves, (e) $d+s$ wave and (f) an anisotropic s-wave gap, respectively. The inset in (f) shows a fourfold symmetric gap function $\Delta(\theta) = 0.72 + 0.18\cos 4\theta$ meV yielded from the fitting with an anisotropic s-wave gap.

are too sharper than the experimental data. Considering possible multi-band in this compound, we also used two mixed components ($s_1 + s_2$ wave or $s + d$ wave) to fit the experimental data (Figs. 3(d) and 3(e)). The double s-wave fitting yields a mixture of 80% of differential conductance value from s_1-wave and 20% from s_2-wave, with $\Delta_{s_1} = 0.80$ meV, $\Gamma_{s_1} = 0.07$ meV and $\Delta_{s_2} = 0.55$ meV, $\Gamma_{s_2} = 0.05$ meV. The $s + d$ wave fitting yields a mixture of 50% d-wave and 50% s-wave, with $\Delta_d = 0.80$ meV, $\Gamma_d = 0.03$ meV and $\Delta_s = 0.85$ meV, $\Gamma_s = 0.03$ meV. The fittings are better than those by one gap as shown in Figs. 3(b) and 3(c), but still not perfect. For the (001)-oriented surface being fourfold symmetric, fitting the spectrum using an anisotropic s-wave gap with fourfold symmetry is reasonable. For the anisotropic s-wave model expressed as $\Delta(\theta) = \Delta_1 + \Delta_2 \cos 4\theta$, the theoretical function can fit the experimental data perfectly and catch the features of both the coherence peaks and the bottom. The best fitting leads to $\Delta_1 = 0.72$ meV, $\Delta_2 = 0.18$ meV, and $\Gamma = 0.058$ meV. The inset

of Fig. 3(f) shows the resultant cruciate-flower-shaped gap function with a maximum of 0.90 meV and a minimum of 0.54 meV. Taking the average gap value we determine $2\Delta_1/k_BT_c \approx 3.55$ which is close to 3.53 predicted by Bardeen-Cooper-Schrieffer (BCS) theory in the weak coupling regime. It should be noted that the spectrum measured at the lowest temperature 0.4 K shows very small but finite ungapped LDOS near zero-bias, however the 'U' shape instead of 'V' shape of the spectrum bottom in addition with the fitting results reduces the possibility of the nodes in the gap function. The finite differential conductance can be described well by the broadening parameter Γ which is related to other broadening effects except temperature. For example, lifetime effect in superconducting granular aluminum can lift the zero-bias conductance to finite value even at 60 mK ($3\%T_c$)[48]. In $(Pb_{0.5}Sn_{0.5})_{0.7}In_{0.3}Te$ sample, there may be some scattering effect in the bulk or on the surface which causes such 7% zero-bias LDOS at 400 mK.

Fig. 4(a) shows the temperature dependence of tunneling spectra measured from 0.4 K to 5 K as symbols. From a deep groove-like structure, the superconducting feature evolves into a shallow with the increase of the temperature and finally disappears at 5 K which is above T_c. We also fitted the temperature dependent spectra with Dynes model by anisotropic s-wave gaps with fixed Δ_1/Δ_2 and using experimental temperature as the parameter. These fittings consist well with the experimental data. The maximum gap values $\Delta_{max} = \Delta_1 + \Delta_2$ obtained by fitting are plotted in Fig. 4(b). The solid line in Fig. 4(b) is obtained through the numerical solution to the BCS gap equation by fixing the $\Delta_{max}(0) \approx \Delta_{max}(T = 0.4\,\mathrm{K}) = 0.9$ meV and $T_c = 4.7$ K derived from Fig.2(b). We can find that the temperature dependent energy gap from the fitting can be described well by the BCS model.

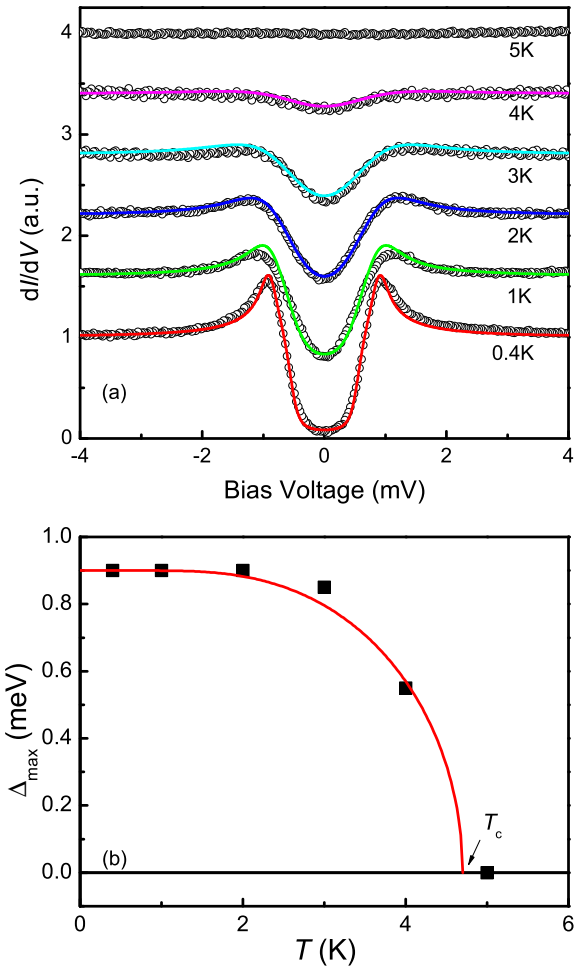

FIG. 4: (color online) (a) Temperature dependence of tunneling spectra measured from 0.4 K to 5 K (symbols) and theoretical fittings (solid lines) by anisotropic s-wave gaps. (b) Temperature dependence of maximal gap ($\Delta_1+\Delta_2$) value derived by the fittings. The solid line is the result of theoretical calculation using BCS model by fixing $\Delta_{max}(0)$ and T_c derived from our experiment (see text).

We notice that several groups have applied point contact measurements on some candidates of TSC such as $Cu_xBi_2Se_3$ and $Sn_{1-x}In_xTe$ single crystals. Zero-bias conductance peaks were detected[12,13,32] and were interpreted in terms of nontrivial topological superconductivity[19,32]. However, due to the complexity of the junctions in point contact experiments, such kind of zero-bias peaks can be induced by several mechanisms other than Majorana modes. The STS spectra we measured are fully gapped without any in gap states, which is different from the point contact measurements in other materials mentioned above. Similarly, Levy et al. applied STM experiments on $Cu_xBi_2Se_3$ single crystals[17], and a fully gapped superconducting gap was also observed. Another interesting result on $Cu_xBi_2Se_3$ shows that the zero bias peaks observed in point contact experiments depend on the barrier transparency and they may not represent the intrinsic feature of the compound[16]. Although $Sn_{1-x}In_xTe$ is a candidate of TSC according to theory[32], a recent thermal conductivity measurement proves that this compound has a full superconducting gap in the bulk[33]. Another group studied $Sn_{1-x}In_xTe$ ($x = 0.38 \sim 0.45$) using muon-spin spectroscopy, and the results can be well described by a single-gap s-wave BCS model[34]. These results have reduced the possibility of being a TSC for $Sn_{1-x}In_xTe$. $(Pb_{1-z}Sn_z)_{1-x}In_xTe$ and $Sn_{1-x}In_xTe$ share the same crystal structure, and with our results reported here, we conclude that the superconductivity in $(Pb_{0.5}Sn_{0.5})_{0.7}In_{0.3}Te$ is topologically trivial and even conventional. Since our present study is based on a top layer with the (001) orientation, we cannot exclude the possibility of topological surface state at the surfaces with the (011) and (111) orientations, which will stimulate the effort in the future.

In summary, we report the first set data of temperature dependent scanning tunneling spectroscopy on $(Pb_{0.5}Sn_{0.5})_{0.7}In_{0.3}Te$, a possible candidate of the topo-

logical superconductor. The low temperature spectrum shows the fully-gapped feature without any in-gap states, and it can be fitted well by an anisotropic s-wave gap using Dynes model. Combining with previous experiments in $Sn_{1-x}In_xTe$ with the same structure, we conclude that the (001)-oriented surface we detected in $(Pb_{0.5}Sn_{0.5})_{0.7}In_{0.3}Te$ does not show evidence of topological superconducting state, although the bulk $Pb_{0.5}Sn_{0.5}Te$ has been proved to be a topological crystalline insulator.

We appreciate the useful discussions with Qianghua Wang and the useful help of using the Laue diffraction machine by Jianzhong Liu. This work was supported by the Ministry of Science and Technology of China (973 projects: 2011CBA00102, 2012CB821403), NSF of China and PAPD. Work at Brookhaven is supported by the Office of Basic Energy Sciences, Division of Materials Sciences and Engineering, U.S. Department of Energy under Contract No. DE-SC00112704. RZ and JS are also supported as part of the Center for Emergent Superconductivity, an Energy Frontier Research Center funded by the U.S. Department of Energy, Office of Science.

* Electronic address: huanyang@nju.edu.cn,hhwen@nju.edu.cn

[1] X. L. Qi and S. C. Zhang, Rev. Mod. Phys. **83**, 1057 (2011).
[2] A. Y. Kitaev, Ann. Phys. (Amsterdam) **303**, 2 (2003).
[3] L. Fu and C. L. Kane, Phys. Rev. Lett. **100**, 096407 (2008).
[4] M. X. Wang, C. H. Liu, J. P. Xu, F. Yang, L. Miao, M. Y. Yao, C. L. Gao, C. Y. Shen, X. C. Ma, X. Chen, Z. A. Xu, Y. Liu, S. C. Zhang, D. Qian, J. F. Jia, and Q. K. Xue, Science **336**, 52 (2012)
[5] E. Wang, H. Ding, A. V. Fedorov, W. Yao, Z. Li, Y. F. Lv, K. Zhao, L. G. Zhang, Z. Xu, J. Schneeloch, R. D. Zhong, S. H. Ji, L. L. Wang, K. He, X. C. Ma, G. D. Gu, H. Yao, Q. K. Xue, X. Chen, and S. Y. Zhou, Nat. Phys. **9**, 621 (2013).
[6] J. P. Xu, C. H. Liu, M. X. Wang, J. F. Ge, Z. L. Liu, X. J. Yang, Y. Chen, Y. Liu, Z. A. Xu, C. L. Gao, D. Qian, F. C. Zhang, and J. F. Jia, Phys. Rev. Lett. **112**, 217001 (2014).
[7] Z. Z. Li, F. C. Zhang, and Q. H. Wang, Sci. Rep. **4**, 6363 (2014).
[8] J. P. Xu, M. X. Wang, Z. L. Liu, J. F. Ge, X. J. Yang, C. H. Liu, Z. A. Xu, D. D. Guan, C. L. Gao, D. Qian, Y. Liu, Q. H. Wang, F. C. Zhang, Q. K. Xue, and J. F. Jia, Phys. Rev. Lett. **114**, 017001 (2015).
[9] M. Z. Hasan and C. L. Kane, Rev. Mod. Phys. **82**, 3045 (2010).
[10] Y. S. Hor, A. J. Williams, J. G. Checkelsky, P. Roushan, J. Seo, Q. Xu, H.W. Zandbergen, A. Yazdani, N. P. Ong, and R. J. Cava, Phys. Rev. Lett. **104**, 057001 (2010).
[11] L. Fu and E. Berg, Phys. Rev. Lett. **105**, 097001 (2010).
[12] S. Sasaki, M. Kriener, K. Segawa, K. Yada, Y. Tanaka, M. Sato, and Y. Ando, Phys. Rev. Lett. **107**, 217001 (2011).
[13] T. Kirzhner, E. Lahoud, K. B. Chaska, Z. Salman, and A. Kanigel, Phys. Rev. B **86**, 064517 (2012).
[14] T. H. Hsieh and L. Fu, Phys. Rev. Lett. **108**, 107005 (2012).
[15] A. Yamakage, K. Yada, M. Sato, and Y. Tanaka, Phys. Rev. B **85**, 180509 (2012).
[16] H. B. Peng, D. De, B. Lv, F. Y. Wei, and C. W. Chu, Phys. Rev. B **88**, 024515 (2013).
[17] N. Levy, T. Zhang, J. Ha, F. Sharifi, A. A. Talin, Y. Kuk, and J. A. Stroscio, Phys. Rev. Lett. **110**, 117001 (2013).
[18] L. Fu, Phys. Rev. Lett. **106**, 106802 (2011).
[19] T. H. Hsieh, H. Lin, J. Liu, W. Duan, A. Bansil, and L. Fu, Nat. Commun. **3**, 982 (2012)
[20] Y. Tanaka, Z. Ren, T. Sato, K. Nakayama, S. Souma, T. Takahashi, K. Segawa, and Y. Ando, Nat. Phys. **8**, 800 (2012).
[21] S. Y. Xu, C. Liu, N. Alidoust, M. Neupane, D. Qian, I. Belopolski, J. D. Denlinger, Y. J. Wang, H. Lin, L. A. Wray, G. Landolt, B. Slomski, J. H. Dil, A. Marcinkova, E. Morosan, Q. Gibson, R. Sankar, F. C. Chou, R. J. Cava, A. Bansil, and M. Z. Hasan, Nat. Commun. **3**, 1192 (2012).
[22] S. Safaei, P. Kacman, and R. Buczko, Phys. Rev. B **88**, 045305 (2013).
[23] P. Dziawa, B. J. Kowalski, K. Dybko, R. Buczko, A. Szczerbakow, M. Szot, E. Łusakowska, T. Balasubramanian, B. M. Wojek, M. H. Berntsen, O. Tjernberg, and T. Story, Nat. Mater. **11**, 1023 (2012).
[24] B. M. Wojek, R. Buczko, S. Safaei, P. Dziawa, B. J. Kowalski, M. H. Berntsen, T. Balasubramanian, M. Leandersson, A. Szczerbakow, P. Kacman, T. Story, and O. Tjernberg, Phys. Rev. B **87**, 115106 (2013).
[25] I. Pletikosić, G. D. Gu, and T.Valla, Phys. Rev. Lett. **112**, 146403 (2014).
[26] Y. Tanaka, T. Sato, K. Nakayama, S. Souma, T. Takahashi, Z. Ren, M. Novak, K. Segawa, and Y. Ando, Phys. Rev. B **87**, 155105 (2013).
[27] S. Safaei, P. Kacman, and R. Buczko, Phys. Rev. B **88**, 045305 (2013).
[28] J. W. Liu, W. H. Duan, and L. Fu, Phys. Rev. B **88**, 241303(R) (2013).
[29] Y. J. Wang, W. F. Tsai, H. Lin, S. Y. Xu, M. Neupane, M. Z. Hasan, and A. Bansil, Phys. Rev. B **87**, 235317 (2013).
[30] R. D. Zhong, J. A. Schneeloch, X. Y. Shi, Z. J. Xu, C. Zhang, J. M. Tranquada, Q. Li, and G. D. Gu, Phys. Rev. B **88**, 020505(R) (2013).
[31] G. Balakrishnan, L. Bawden, S. Cavendish, and M. R. Lees, Phys. Rev. B **87**, 140507(R) (2013)
[32] S. Sasaki, Z. Ren, A. A. Taskin, K. Segawa, L. Fu, and Y. Ando, Phys. Rev. Lett. **109**, 217004 (2012).
[33] L. P. He, Z. Zhang, J. Pan, X. C. Hong, S. Y. Zhou, and S. Y. Li, Phys. Rev. B **88**, 014523 (2013).
[34] M. Saghir, J. A. T. Barker, G. Balakrishnan, A. D. Hillier, and M. R. Lees, Phys. Rev. B **90**, 064508 (2014).
[35] G. S. Bushmarina, I. A. Drabkin, D. V. Mashovets, R. V. Parfeniev, D. V. Shamshur, and M. A. Shachov, Physica B **169**, 687 (1991).
[36] R. V. Parfenév, D. V. Shamshur, M. A. Shakhov, and Zb. Chrapkiewicz, J. Alloys Compd. **219**, 313 (1995).
[37] R. V. Parfenév, D. V. Shamshur, and S. A. Nemov, Phys. Solid State **43**, 1845 (2001).
[38] J. R. Dixon and R. F. Bis, Phys. Rev. **176**, 942 (1968).
[39] B. M. Vul, I. D. Voronova, G. A. Kalyuzhnaya, T. S.

Mamedov, and T. Sh. Ragimova, JETP Lett. **29**, 18 (1979).
[40] V. I. Kozub, R. V. Parfenév, D. V. Shamshur, D. V. Shakura, A. V. Chernyaev, and S. A. Nemov, JETP Lett. **84**, 35 (2006).
[41] D. V. Shamshur, S. A. Nemov, R. V. Parfenév, M. S. Kononchuk, and V. I. Nizhankovskii, Phys. Solid State **50**, 2028 (2008).
[42] R. D. Zhong, J. A. Schneeloch, T. S. Liu, F. E. Camino, J. M. Tranquada, and G. D. Gu, Phys. Rev. B **90**, 020505(R) (2014).
[43] Ø. Fischer, M. Kugler, I. Maggio-Aprile, C. Berthod, and C. Renner, Rev. Mod. Phys. **79**, 353 (2007).
[44] J. E. Hoffman, Rep. Prog. Phys. **74**, 124513 (2011).
[45] Y. Okada, M. Serbyn, H. Lin, D. Walkup, W. W. Zhou, C. Dhital, M. Neupane, S. Xu, Y. J. Wang, R. Sankar, F. C. Chou, A. Bansil, M. Z. Hasan, S. D. Wilson, L. Fu,and V. Madhavan, Science **341**, 1496 (2013).
[46] I. Zeljkovic, Y. Okada, C. Y. Huang, R. Sankar, D. Walkup, W. W. Zhou, M. Serbyn, F. C. Chou, W. F. Tsai, H. Lin, A. Bansil, L. Fu, M. Z. Hasan, and V. Madhavan, Nat. Mater. **10**, 572 (2014).
[47] I. Zeljkovic, Y. Okada, M. Serbyn, R. Sankar, D. Walkup, W. W. Zhou, J. Liu, G. Chang, Y. J. Wang, M. Z. Hasan, F. C. Chou, H. Lin, A. Bansil, L. Fu, and V. Madhavan, Nat. Mater. **14**, 318 (2015).
[48] R. C. Dynes, J. P. Garno, G. B. Hertel, and T. P. Orlando, Phys. Rev. Lett. **53**, 2437 (1984).